Virtual Damping and Einstein Relation in Oscillators

Donhee Ham, *Member, IEEE* and Ali Hajimiri, *Member, IEEE*

Abstract— **This paper offers a new viewpoint to oscillator noise, bringing transparent insight into the phase noise. Built around the well-known concept of phase diffusion, this work bridges fundamental physics of noise and existing oscillator phase noise theories. The concept of virtual damping is presented as a measure of phase noise utilizing an ensemble of oscillators. The explanation of the linewidth compression through virtual damping provides a unified view of resonators and oscillators. The direct correspondence between phase noise and the Einstein relation is demonstrated, illuminating underlying physics of phase noise. The validity of this new approach is positively confirmed by consistent experimental agreement.**

Keywords— **oscillators, resonators, *LC* oscillators, ring oscillators, integrated circuits, analog integrated circuits, radio-frequency (RF) circuits, phase noise.**

I. Introduction

OSCILLATOR phase noise has been studied from several different angles, ranging from a mathematical physics treatment [1] - [4] to CAD-oriented methods [5] [6] and design-oriented approaches [7] - [12], to name a few. The design-oriented approaches have evolved from a familiar linear time-invariant approach [7] to a more accurate time-varying theory [12], adding additional insight into the oscillator design. These studies have helped circuit designers understand the evolution of noise in oscillators, leading to more accurate phase noise predictions, and lower noise designs (*e.g.*, [13] [14]). However, the currently available works on the phase noise assume rather phenomenological or pure mathematical standpoints and a more fundamental, yet intuitive understanding of the phase noise phenomenon is still needed.

The primary goal of this paper is to provide essential physical understanding of the phase noise. This work develops a framework with a supporting measurement that fills in the gap between the fundamental physics of noise and the existing phase noise theories. Based on thought experiments and fundamental arguments, this theory emphasizes a simple, physical picture of phase noise. The results are commensurate with the time-varying theory in [12], but the different emphasis leads to several new insights. The specific contributions and outline of the paper are listed below.

Donhee Ham is with Electrical Engineering, Harvard University, Cambridge, MA 02138, USA. email: donhee@deas.harvard.edu.

Ali Hajimiri is with Electrical Engineering, California Institute of Technology, Pasadena, CA 91125, USA. email: hajimiri@caltech.edu.

A. Organization and Contributions

Section II *reviews* phase noise from the perspective of phase diffusion based on the original contributions in [1] - [4].

The new contributions are presented from Section III on. In Section III, we introduce the concept of *virtual damping* through a thought experiment. We show that virtual damping is another manifestation of phase diffusion and demonstrate the virtual damping rate as a fundamental measure of phase noise, both theoretically and experimentally. The virtual damping concept will enable us to view oscillators and resonators in a unified framework, leading to a deep and intuitive understanding of *linewidth compression*.

Section IV derives the virtual damping rate in terms of circuit parameters in a general time-varying case. The derivation using the diffusion equation explains intuitively how the time-varying effects physically modify the virtual damping rate but why we never directly observe the time-variations themselves in phase noise measurement.

In Section V, we give a physical interpretation of the virtual damping rate, revealing the direct correspondence between the Einstein relation and phase noise. This interpretation elucidates the underlying physics of phase noise by identifying its two key elements, *sensitivity* and *energy loss*. The fundamental argument also establishes a link between existing dissipation-based phase noise models (*e.g.*, [7]) and fluctuation-based phase noise models (*e.g.*, [12]).

Finally, Section VI combines the results from the previous sections to calculate the ratio of the resonator's linewidth to the oscillator's linewidth. The anatomy of this linewidth compression in conjunction with the phase noise physics of Section V will form a simple, yet essential perspective of the oscillator phase noise.

II. Review of Phase Noise Fundamentals

In this section, we *review* phase noise fundamentals from the viewpoint of *phase diffusion*. This review is based on the original works presented in [1] - [4] in which central concepts and equations of this section are found (perhaps apart from certain notational differences). Essentially the same equations have reappeared in numerous subsequent developments to analyze phase noise (*e.g.*, [6], [15], and [16], to name a few). We will refer only to original source(s) in this section.

The phase diffusion concept reviewed in this section will be crucial in understanding our contributions presented from Section III on. Since the treatments in currently available phase diffusion literature are often very mathe-
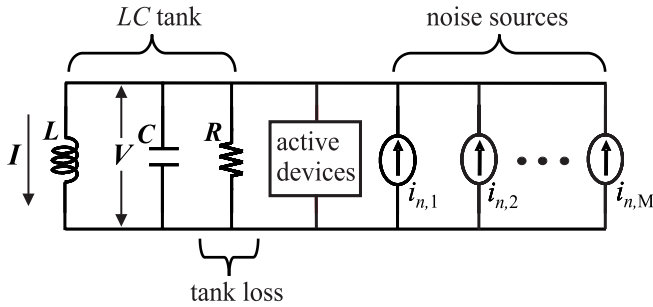
Fig. 1. Generic model for the self-sustained LC oscillator.
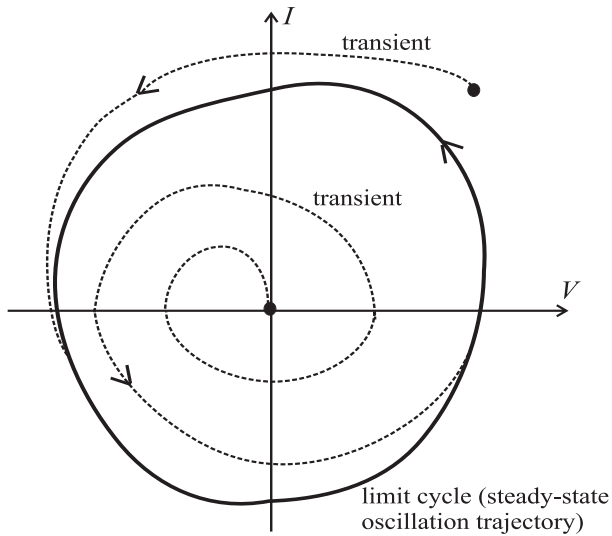
Fig. 2. Limit cycle in the V-I state-space.

Fig. 3. Ensemble of N identical oscillators.

matical, we have made this section rather self-contained, emphasizing intuitive understanding.

A. Phase Diffusion

Self-sustained oscillators are realized by combining some sort of frequency selection mechanism and positive active feedback. For example, an LC oscillator is derived by placing the LC resonator in a positive feedback loop with gain larger than 1. Figure 1 depicts a generic model for the LC oscillator. The resistance, R, represents the parasitic tank loss. The active devices form the positive feedback loop, which compensates the tank loss by converting dc energy to ac energy and injecting it into the LC tank. The oscillation frequency, ω_0, is given by $\omega_0 = 1/\sqrt{LC}$. The tank loss and the active devices generate noise, which are modeled as the current sources in Fig. 1.

The dynamics of an LC oscillator can be visualized by mapping the voltage, V, across the capacitor and the current, I, of the inductor onto a trajectory in the V-I state-space as shown in Fig. 2. For a stable oscillator, the limit cycle representing the steady-state oscillation is a closed curve due to the periodicity [17]. Regardless of its starting point, the state will be ultimately attracted to the limit cycle after the initial transient fades away, as shown in Fig. 2.
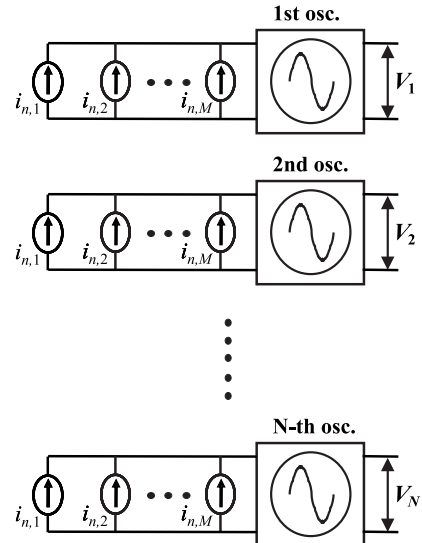
This peculiar property of the self-sustained oscillator directly affects its fluctuation behavior in the presence of noise. The fluctuations would remain small in the radial (amplitude) direction due to the tendency of the state to return to the limit cycle. However, fluctuations in the direction along the limit cycle do not experience any restoring force to return the phase to its original value. Consequently, in the presence of noise, the state point *walks randomly* along the limit cycle, or, the phase undergoes a "diffusion" process [1] - [4].

To see this *phase diffusion* more clearly, let us run a thought experiment using an ensemble of N identical oscillators as in Fig. 3 where N is a very large number. All the oscillators are assumed to be at the same initial phase of zero at $t = 0$. In the state-space picture shown in Fig. 4(a), the state points from the ensemble are all on the top of one another initially, rotating on the limit cycle together. However, the rotating oscillation points diffuse along the limit cycle with time, eventually spreading all over the limit cycle. This implies that the oscillator will completely lose its initial phase information after a sufficiently long time.

In the time-domain, the fundamental component of the voltage across the LC tank in Fig. 1 is expressed as

$$V(t) = V_0 \cos[\omega_0 t + \phi(t)] \qquad (1)$$

where V_0 is the amplitude of the fundamental component. We ignored the amplitude noise since it remains relatively small as discussed shortly before. The fluctuation along the direction of the limit cycle in the state-space corresponds to the phase fluctuation, $\phi(t)$, in (1), which assumes a diffusion process, as mentioned earlier. The time-domain picture of this phase diffusion is shown in Fig. 4(b). Initially, the oscillator output signals from the ensemble are all on the top of one another since the oscillators are at the same initial phase. After a sufficiently long time, however, the output signals become incoherent due to the phase diffusion and eventually go totally "out of sync".
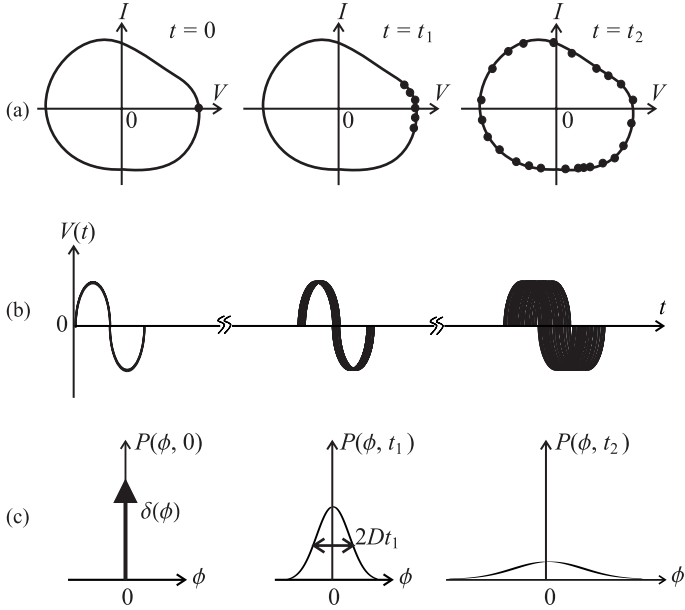
Fig. 4.   (a) Phase diffusion in the state-space. (b) Phase diffusion in the time-domain. (c) Time evolution of $P(\phi, t)$. In all cases, $t_1 < t_2$.

Based on the ensemble, we can define the time-dependent probability distribution of the phase, $P(\phi, t)$. By definition, $P(\phi, t)d\phi$ represents the probability for the phase to be in $(\phi, \phi + d\phi)$ for a given time, t. Figure 4(c) shows the evolution of $P(\phi, t)$ with time. Since all the oscillators in the ensemble are at the same initial phase of zero, the initial distribution is given by $P(\phi, t = 0) = \delta(\phi)$ where $\delta(\phi)$ is the Dirac delta. As time elapses, the phase undergoes diffusion and the probability distribution of ϕ spreads out. As demonstrated in [1] - [4], if the phase diffusion is due to white noise, the variance of ϕ, which signifies the width of the probability distribution, is given by

$$\langle \phi^2(t) \rangle = 2Dt \qquad (2)$$

a key signature of any diffusion process subject to white noise[1] [18] [19]. The validity of (2) in the general time-varying case will be positively confirmed in Section IV. Extensive discussion of (2) is also found in [20] - [22] in the special context of timing jitters in ring oscillators. The constant, D, called *phase diffusion constant*, indicates how fast the phase diffusion occurs.[2] As will be seen shortly, this phase diffusion constant will be the *sole* factor that determines the oscillator phase noise.

In Fig. 4(a) and (b), D is a measure of how fast the oscillator loses its initial phase information or how fast the ensemble evolves to the ultimately chaotic state (the maximum entropy state) at $t = \infty$. Therefore, D can be also thought of as the *entropy-growth-rate*. For instance, an

[1]a.k.a., Wiener process

[2]Although D is a notation traditionally used for the diffusion constant, different notations are often found in the existing literature. For example, in [1], W is used as an indicator of the diffusion rate where $D = W/2$. The constant, κ, used in the context of timing jitters in [21] and [22] is related to D through $D = \kappa^2 \omega_0^2 / 2$.

atomic clock is a system in which the entropy grows extremely slowly.

While the phase diffusion is the fundamental phenomenon solely responsible for the oscillator phase noise, the phase noise is usually characterized in terms of the oscillator power spectrum broadening due to its ease of measurement. Indeed the spectrum broadening is a natural outcome of the phase diffusion. In the following subsection, we will discuss this relation between phase diffusion and phase noise (spectrum broadening).

B. Phase Noise

As shown in [1] - [4], when the oscillator phase, $\phi(t)$, is a diffusion process satisfying (2) subject to white noise, the power spectral density of $V(t)$ in (1) is given by the familiar Lorentzian:

$$S_V(\omega) = V_0^2 \frac{D}{(\Delta\omega)^2 + D^2} \qquad (3)$$

where $\Delta\omega \equiv \omega - \omega_0$ is called the offset frequency from the carrier. Note that regardless of the value of D the total oscillation energy remains the same value, $V_0^2/2$, as can be seen by integrating $S_V(\omega)$ over the whole frequency range.

Figure 5 shows $S_V(\omega)$ versus ω for different phase diffusion constants for the fixed oscillator energy of $V_0^2/2$. For a larger D, the Lorentzian shape is shorter and fatter, distributing the same oscillation energy (the area under the power spectrum curves) more widely around the center frequency, hence increasing the errors in the reference frequency. This is the frequency domain meaning of the phase diffusion constant, D.

The degree of this energy spreading about the center frequency for a given total energy is characterized by phase noise. The phase noise at a given offset frequency, $\Delta\omega$, is defined as the ratio of the power spectral density at the frequency of[3] $\omega_0 + \Delta\omega$ to the total oscillation energy, $V_0^2/2$, [23], which is given by

$$\mathcal{L}\{\Delta\omega\} \equiv \frac{S_V(\omega)}{V_0^2/2} = \frac{2D}{(\Delta\omega)^2 + D^2} \qquad (4)$$

This definition of phase noise is widely-used due to its ease of measurement using common instruments such as spectrum analyzers. If the offset frequency is large enough as compared to D, *i.e.*, for $\Delta\omega \gg D$, (4) assumes a familiar f^{-2} behavior [7]:

$$\mathcal{L}\{\Delta\omega\} \approx \frac{2D}{(\Delta\omega)^2} \qquad (5)$$

We have to emphasize once again that *the phase noise solely depends upon the phase diffusion constant, D.* In other words, the phase diffusion constant is a direct measure of the phase noise. A slower phase diffusion corresponds to a smaller spectrum broadening in the frequency domain.

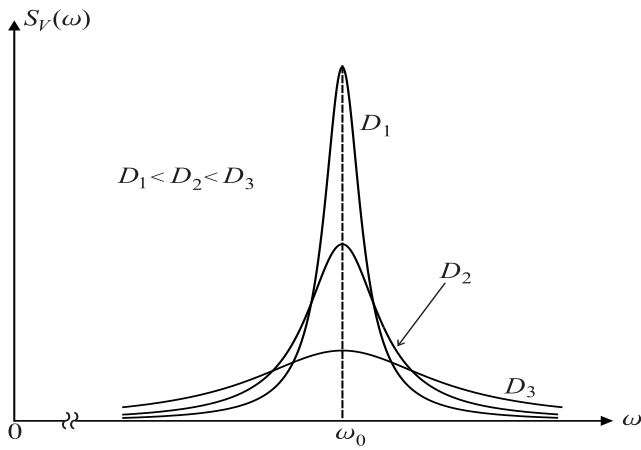[3]Or alternatively, at $\omega_0 - \Delta\omega$

Fig. 5. Power spectral densities of the oscillator output for different diffusion constants for the same oscillation energy.

Fig. 6. Ensemble average of $V(t)$ and virtual damping.

III. VIRTUAL DAMPING

The previous section reviewed phase noise fundamentals based on [1] - [4]. The rest of this paper presents our work on phase noise, beginning with the *virtual damping* in this section.

A. Virtual Damping Concept

To derive the virtual damping concept, we resort to the thought experiment of Fig. 3 again that involves the ensemble of identical oscillators. Time-domain picture of the phase diffusion was depicted in Fig. 4(b) using the ensemble of oscillators and is redrawn at the top of Fig. 6. Initially, the oscillators in the ensemble have the same phase and hence the ensemble average, $\langle V(t)\rangle$, is equal to $V(t)$ of any single oscillator in the ensemble. After a sufficiently long time, however, the oscillator signals become incoherent due to the phase diffusion and hence $\langle V(t)\rangle$ tends to zero with time, as shown at the bottom of Fig. 6. We refer to this damping of the ensemble average as *virtual damping*. Even though the single oscillator output, $V(t)$, *per se* sustains itself, its ensemble average which matters in the measurement of phase noise *virtually damps*. One can intuitively guess that the phase diffusion constant, D, is associated with the virtual damping rate: a slower phase diffusion is expected to result in a slower virtual damping.

A quantitative verification of the virtual damping is given here. For a Gaussian distribution of ϕ, $\langle\cos\phi\rangle = e^{-\langle\phi^2\rangle/2}$ and $\langle\sin\phi\rangle = 0$ [18]. In the presence of white noise, the oscillator phase, $\phi(t)$, satisfies (2), and hence ensemble average of $V(t)$ in (1) is given by

$$\langle V(t)\rangle = V_0 e^{-\langle\phi^2(t)\rangle/2}\cos(\omega_0 t) = V_0 e^{-Dt}\cos(\omega_0 t) \qquad (6)$$

which clearly shows the virtual damping. The virtual damping assumes an exponential behavior and *the virtual damping rate is identical to the phase diffusion constant, D*, as we guessed earlier. From the mathematical perspective, (6) *per se* is not surprisingly new as it results from the standard probability calculation similar to the one shown
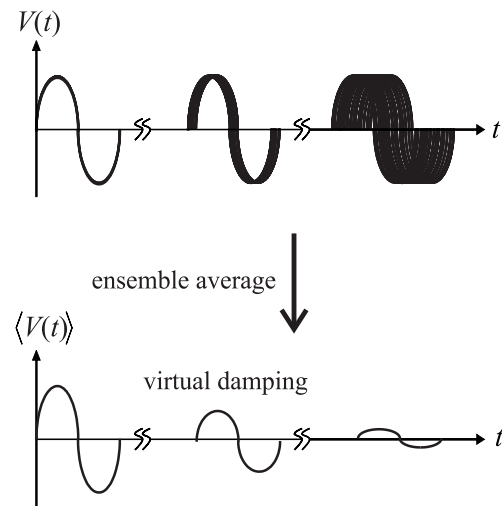
in [24], which alone does not necessarily provide a physical meaning in conjunction with phase diffusion or its far-reaching implications. However, the virtual damping concept indeed has far-reaching implications, leading to an intuitive understanding of phase noise in a unified framework where resonators and oscillators are viewed from the same angle, as will be seen shortly.

$1/D$ (time constant)	# of cycles within $1/D$	phase noise (dBc/Hz)
1 millisecond	1.0×10^6	-99
1 second	1.0×10^9	-129
1 minute	6.0×10^{10}	-146
1 hour	3.6×10^{12}	-164
1 day	8.6×10^{13}	-178
1 month	2.6×10^{15}	-193
1 year	3.1×10^{16}	-203

Table 1. Phase noise of a 1 GHz oscillator at 600 kHz offset for different values of D obtained using (5). The white noise floor of the real measurement system is being ignored.

The virtual damping rate, D, and the phase noise of the oscillator are related through (5). To get a feel for the size of the virtual damping rate, let us consider an example: a 1 GHz RF oscillator whose phase noise is -121dBc/Hz at 600 kHz offset has $D \approx 5.6$ Hz or $D/f_0 \sim 10^{-9}$ according to (5). As this numerical example shows, *typical oscillators have very slow virtual damping rates when compared to oscillation frequencies*. The time constant, $1/D$, associated with this particular virtual damping is approximately 0.2 seconds and phase errors will be apparent after this amount of time. Within this time constant, there are approximately 10^8 oscillation cycles.

More numerical examples are tabulated in Table 1, which lists phase noise values of a 1 GHz RF oscillator at 600 kHz offset for different virtual damping rates. All the phase noise values are calculated using (5) and some of the smaller values cannot be measured in the practical measurement due to the white noise floor of the measurement system. As

can been seen, currently available silicon-based on-chip oscillators whose phase noise values range typically between -100 dBc/Hz and -140 dBc/Hz at the offset frequency (*e.g.,* [13], [14], [25] - [31]) have virtual damping time constants roughly between milliseconds and seconds.

B. Experimental Verification

We can observe the virtual damping phenomenon experimentally as well. Typical *LC* oscillators have very slow virtual damping rates as compared to the oscillation frequency, making them less suitable for experimental verification. Instead, we use ring oscillators whose phase noise is significantly degraded by injection of a white noise current whose power spectrum can be controlled externally. However, we must emphasize that the exponential virtual damping is a general phenomenon in any types of oscillators influenced by white noise, as the generic mathematical model in the previous subsection suggests.

The experimental setup is shown in Fig. 7. The ring oscillator is obtained by placing a cascade of five inverter stages in a feedback loop. The oscillation frequency is controlled by adjusting the supply voltage, V_{dd}. The externally injected noise is generated by an HP33120A arbitrary waveform generator and has a white spectrum across the bandwidth of interest. This bandwidth refers to the frequency band within which the spectrum of the oscillator is above the noise floor and phase noise is measurable.

A Tektronix TDS3054 digital oscilloscope is used to sample the output waveform multiple times and calculate the average over N samples, *i.e.,* $\langle V(t)\rangle_N$. The N output waveforms are triggered at the same phase at $t = 0$. To make this average as close to the mathematical ensemble average as possible, a considerably large N of 512 was chosen and the environmental parameters such as temperature were maintained as constant as possible throughout the measurement. Under this carefully controlled environmental conditions, the average of the output waveforms from the same oscillator sampled at different time intervals will converge to ensemble average as N increases.[4]

Figure 8 shows this average for 512 samples as a function of time. As can be seen clearly, the average is an exponentially damping sinusoidal even though the single output waveform is a steady-state sinusoidal. This measurement result is in complete agreement with the virtual damping concept and equation (6).

Using this experiment, the virtual damping rate, D, was measured for different injected noise power levels. As (6) indicates, D is the inverse of time constant of the best-fit exponential to the resultant time domain averaged waveform such as the one in Fig. 8. The measured virtual damping rate was used in (5) to predict the phase noise at the 1 MHz offset frequency. The oscillator phase noise was also directly measured at the same offset frequency using an HP8563E spectrum analyzer with phase noise measurement utility. Table 2 summarizes the experimental results.

[4]We assume ergodicity that the time average is equal to the ensemble average, which is a fundamental assumption used in many measurement systems such as spectrum analyzers.
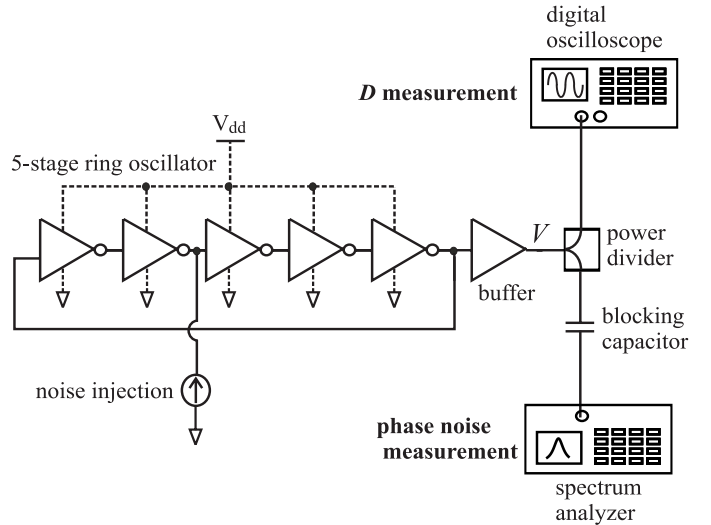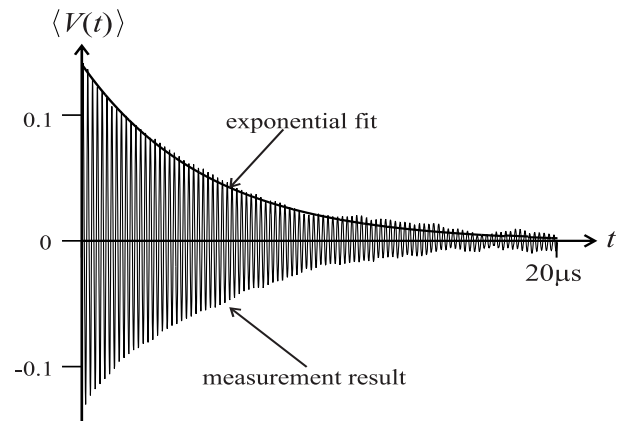

Fig. 7. Measurement setup for the virtual damping.

Fig. 8. A measurement example: measured $\langle V(t)\rangle_{512}$ versus t.

As can be seen, there is close and consistent agreement between the two phase noise measurement methods, hence confirming the validity of the virtual damping concept.

$\overline{i_n^2/\Delta f}$ (A^2/Hz)	Measured D (sec^{-1})	PN from measured D (dBc/Hz)	measured PN (dBc/Hz)
2.6×10^{-15}	1.02×10^{4}	-92.9	-93.0
4.8×10^{-15}	1.56×10^{4}	-91.0	-90.0
9.7×10^{-15}	3.53×10^{4}	-87.4	-86.5
2.1×10^{-14}	9.30×10^{4}	-83.3	-81.7
6.0×10^{-14}	1.90×10^{5}	-80.2	-79.5

Table 2. Measured D, phase noise calculated from the measured D, and phase noise measured using a spectrum analyzer at different injected noise power levels for the ring oscillator whose center frequency was set at 5 MHz. The offset frequency at which the phase noise was measured is 1 MHz.

Apart from the virtual damping, the measurement setup in Fig. 8 also facilitates observation of the full Lorentzian behavior given by (4). For practically usable oscillators,
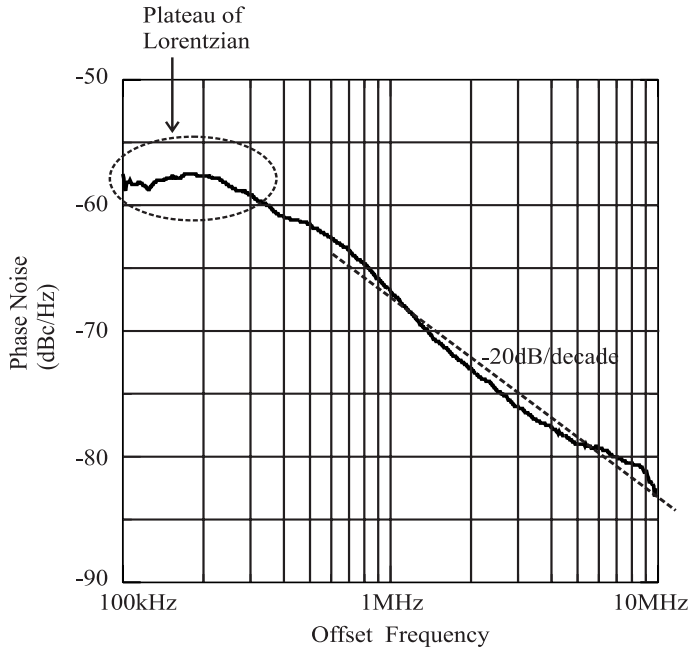
Fig. 9. Measured phase noise vs. offset frequency for a very large D. The Lorentzian shape is apparent.

Fig. 10. Linewidth compression.

the virtual damping rate, D, is very small as compared to the typical offset frequencies (*e.g.*, Table 1), which justifies the widely-used $1/f^2$ approximation in (5) for phase noise characterization. In other words, the plateau of the Lorentzian spectrum predicted by (4) is hard to observe for the typical good oscillators due to their relatively small D. However, in the oscillator of Fig. 8 where D can be made comparable to the typical offset frequencies via injection of external white noise, the full Lorentzian spectrum becomes observable. Figure 9 shows a phase noise measurement example using the spectrum analyzer for a very large D. In the figure, the plateau as well as the familiar -20dB/decade reduction part is apparent, and hence the full Lorentzian spectrum.

C. Linewidth Compression

The virtual damping concept provides a unified framework to view the resonator and the oscillator from the same angle. This subsection will explain this viewpoint, giving a fundamental yet intuitive understanding of linewidth compression (Fig. 10).

The left-hand side of Fig. 10 shows a parallel LC resonator. The energy loss due to the parasitic resistance, R, causes the voltage across the tank to damp exponentially from a given initial value as shown in the figure. This damping in the time-domain corresponds to the line broadening in the energy spectrum in the frequency-domain.

The right-hand side of Fig. 10 shows an oscillator derived from the same LC resonator by driving it in positive active feedback. The phase diffusion due to the active and passive device noise is responsible for the line broadening of oscillator's power spectrum (phase noise) as discussed earlier. Since the virtual damping is another manifestation of the
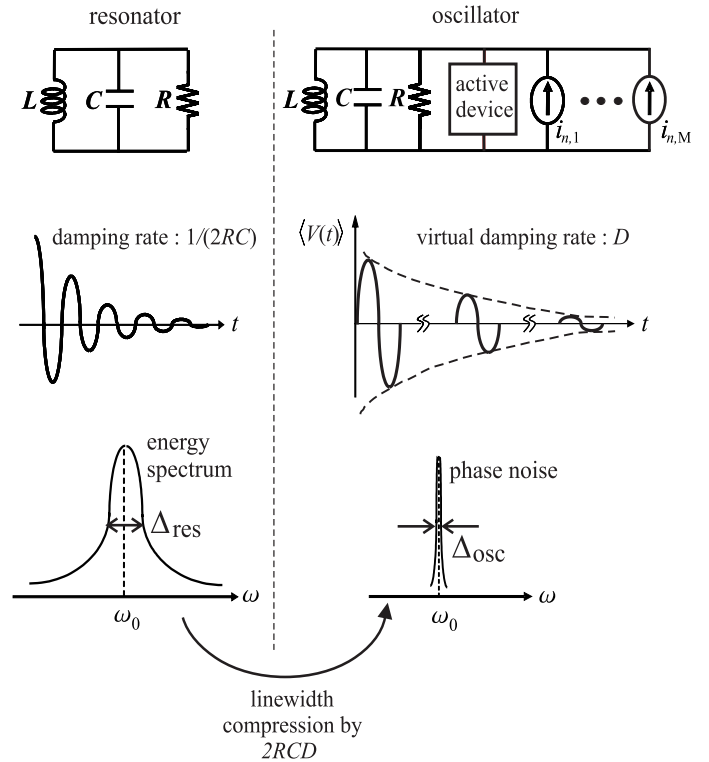
phase diffusion, the line broadening in oscillator's power spectrum can be alternatively thought of as the result of the exponential virtual damping, and henceforth, the virtual damping rate in the time-domain corresponds to the spectrum linewidth in the frequency domain.[5] The virtual damping is extremely slower than the oscillation frequency as discussed earlier and hence it is almost always much slower than the damping in the resonator. Correspondingly, the linewidth of the oscillator's output spectrum is much smaller than the linewidth of the resonator's energy spectrum, as shown hypothetically in Fig. 10.

In conclusion, placing a resonator in a positive feedback loop to make a self-sustained oscillator results in *linewidth compression*. The ratio of the oscillator's virtual damping rate, D, to the resonator's damping rate, $1/(2RC)$, is the measure of this linewidth compression ratio:

$$r \equiv \frac{\Delta_{osc}}{\Delta_{res}} = \frac{D}{1/(2RC)} = \frac{2Q}{\omega_0} \cdot D \qquad (7)$$

where the *unloaded quality factor*, Q, of the LC tank is defined as usual:

$$Q = RC\omega_0 \qquad (8)$$

---

[5]To be the most accurate, the linewidth of the oscillator power spectrum corresponds to the damping rate of the autocorrelation, $\langle V(t)V(t+\tau)\rangle$, as opposed to the virtual damping rate of the mean, $\langle V(t)\rangle$, since the power spectrum is the Fourier transform of the autocorrelation. However, since the virtual damping of the mean and the damping of the autocorrelation are of the same physical origin, the simpler view of relating the virtual damping of the mean to the spectrum linewidth in this paper will serve the essential purpose. Additionally, the damping rate of the autocorrelation calculated in [1] is exactly the same as the virtual damping rate of the mean!

To get a sense for the size of this linewidth compression ratio, let us consider an example of a 1 GHz LC oscillator whose phase noise at 600 kHz offset is -121 dBc/Hz. Let us assume that the LC tank has Q of 10. According to (5), $D \approx 5.6$ Hz and therefore, $r \approx 1.8 \times 10^{-8}$. As can be seen, the linewidth compression ratio for this typical example is extremely small, showing that the linewidth of a resonator is narrowed by almost 8 orders of magnitude when placed in a positive feedback loop to make an oscillator. In the time-domain picture, this observation is equivalent to the fact that the virtual damping rate of the oscillator is 8 orders of magnitude smaller than the damping rate of the resonator.

This linewidth compression concept with the aid of Fig. 10 elucidates that the phase noise of the resonator-based oscillators is optimized by a *two-step procedure*. The first step is to select a resonator with the narrowest possible linewidth. Since the resonator's linewidth is $\Delta_{res} \sim 1/(2RC) = \omega_0/2Q$ where Q is given by (8), this first optimization step is actually equivalent to high-Q resonator selection. The second optimization step is to achieve the highest possible linewidth compression by minimizing r in (7) in placing the resonator in the positive feedback loop. As will be seen in Section VI, the linewidth compression ratio, r, strongly depends on the noise-to-carrier ratio (NCR) defined as [30]

$$\text{NCR} \equiv \frac{E_{thermal}}{E_{tank}} = \frac{k_B T}{C V_0^2} \qquad (9)$$

where $E_{thermal} = k_B T/2$ and $E_{tank} = C V_0^2/2$ are the thermal and tank energy, respectively. Therefore the maximum linewidth compression in the second step may be achieved through the minimization of the NCR.[6]

Each of the two steps described above is well known in the context of phase noise optimization. The first step of optimizing resonator's Q has been a traditional focus in the oscillator design. The second step of the NCR minimization is typically exercised through the oscillation amplitude maximization but there have recently been emphases on the more proper tank energy maximization [26] [30] [32]. However, these two quantities, Q and NCR, have been understood rather separately but not in the context of the two-step procedure, and understanding of how phase noise behaves as a whole depending on both Q and the NCR has been lacking. For instance, the link between the NCR and the phase noise has never been clearly explained, *e.g.*, [30] [32] [33], to the best of our knowledge. The linewidth compression concept addresses this issue, establishing the link between the NCR and the phase noise and leading to a global picture of phase noise.

This understanding of phase noise via linewidth compression will be further enhanced after the study of phase noise physics in Section V with an explicit expression for D in terms of circuit parameters in hand. Section VI will revisit this linewidth compression. The following section derives the virtual damping rate in terms of circuit parameters.

[6]In most practical cases, these two optimization steps are intermingled.

IV. VIRTUAL DAMPING RATE

In order to derive the virtual damping rate, D, we first have to find the governing equation of phase dynamics in the presence of white noise. To this end, let us consider the LC circuit in Fig. 1 and its associated V-I state space and limit cycle in Fig. 11. At time t, the oscillation point is assumed to be at point **A** on the limit-cycle. During an infinitesimal time interval, $(t, t + dt)$, a noise current, i_n, will dump a charge, $i_n dt$, to the capacitor, resulting in the instantaneous voltage change, $dV = i_n dt/C$, across the capacitor, or equivalently the momentary shift of the state point from **A** to **A′** where $\overline{\mathbf{AA′}} = dV$. The perturbed point, **A′**, will eventually return to the limit cycle at point **B′** after traveling along the trajectory shown with the broken curve. During the same amount time, if there were no such perturbation, the state point **A** would travel along the limit cycle to end up at point **B**. This shift from **B** to **B′** is responsible for the phase change, $d\phi$, due to the noise perturbation [5] [12]. For small enough perturbations, $d\phi$ is proportional to dV and is inversely proportional to the oscillation amplitude, V_0. For the same dV, the resultant phase change, $d\phi$, also depends on where the state point was on the limit cycle at the time of the noise injection due to the periodic sensitivity of the state point to the perturbation. We use a unitless periodic function, $\Gamma(t)$, to denote this periodic sensitivity, the so-called impulse sensitivity function (ISF)[7] [12] [34]. Then the governing equation of the phase dynamics can be written as

$$d\phi = \frac{dV}{V_0}\Gamma(t) = \frac{i_n dt}{C V_0}\Gamma(t) = \frac{i_n dt}{q_{max}}\Gamma(t) \qquad (10)$$

where

$$q_{max} \equiv C V_0 \qquad (11)$$

signifies the charge amplitude.

Additionally, the noise source, $i_n(t)$, is cyclostationary in general due to the periodic change of the operating point, and hence should be replaced with $i_n(t)\alpha(t)$ where $i_n(t)$ is stationary noise and $\alpha(t)$ is the unitless periodic noise modulating function (NMF) [12] [34]. Then the generalized version of (10) is given by

$$\frac{d\phi}{dt} = \frac{1}{q_{max}}i_n(t)\Gamma_{eff}(t) \qquad (12)$$

where the unitless periodic function, $\Gamma_{eff}(t) \equiv \alpha(t)\Gamma(t)$, is called effective ISF [12] [34]. As can be seen, the phase, $\phi(t)$, is an integration of the white noise, $i_n(t)$, and hence represents a diffusion process as mentioned earlier several times.

In order to find the phase diffusion constant, D, we derive, from (12), the diffusion equation describing the time evolution of the phase probability distribution, $P(\phi, t)$, introduced in Section II. See Fig. 4(c). This type of conversion is a standard exercise in stochastic theory [18] and in

[7]Analytical evaluation of the ISF is difficult as it involves detailed mechanism how the perturbed state point returns to the limit cycle [6] [12] [34]. In practice, we can use an empirical method to obtain the ISF utilizing charge injection simulation [12] [34].
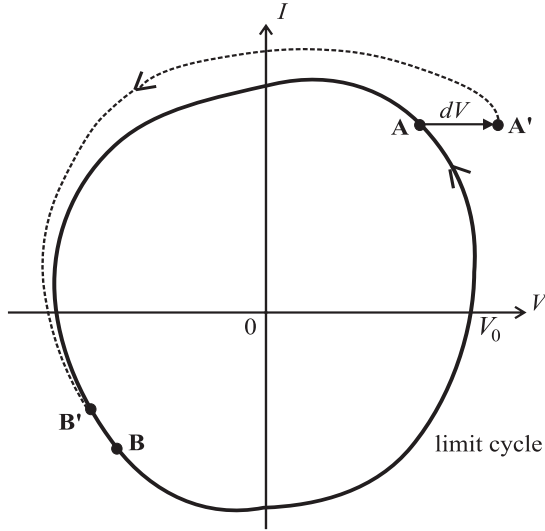
Fig. 11.   Geometric description of phase dynamics.

this special case leads to [35]:

$$\frac{\partial P}{\partial t} = D(t)\frac{\partial^2 P}{\partial \phi^2} \tag{13}$$

where

$$D(t) = \frac{1}{4q_{max}^2} \cdot \frac{\overline{i_n^2}}{\Delta f} \cdot \Gamma_{eff}^2(t) \tag{14}$$

Equation (13) resembles the typical diffusion equation [18] [19] except that the diffusion rate, $D(t)$, is not constant but periodic due to the time-varying effect represented by $\Gamma_{eff}(t)$. Seemingly complicated, it can be rather easily shown that solving the time-varying diffusion equation (13) is equivalent to solving the following typical diffusion equation

$$\frac{\partial P}{\partial t} = \overline{D(t)}\frac{\partial^2 P}{\partial \phi^2} \tag{15}$$

where $\overline{D(t)}$ signifies the time average of $D(t)$ over its fundamental period, or equivalently, its dc component (See Appendix for the proof.). In other words, even in the presence of the periodic time-varying effects, the diffusion occurs with the diffusion constant of $\overline{D(t)}$, or $\langle \phi^2(t) \rangle = 2 \cdot \overline{D(t)} \cdot t$, *as if there were no time-varying effects.* This verifies (2) in the general time-varying case where the phase diffusion constant, or the virtual damping rate, D, is given by

$$D = \overline{D(t)} = \frac{1}{4q_{max}^2} \cdot \frac{\overline{i_n^2}}{\Delta f} \cdot \Gamma_{eff,rms}^2 \tag{16}$$

Here $\Gamma_{eff,rms}$ signifies the root mean square of the effective ISF.

While the phase diffusion itself occurs as if there were no time-varying effects, the shape of the periodic $\Gamma_{eff}(t)$ *does* affect the diffusion speed by modifying the averaged (rms) value in (16). This is essentially because diffusion is an accumulation process: D represents an overall diffusion speed, which is obtained through accumulation of a

large number of phase random walks during numerous oscillation cycles. In this accumulation process, the details of the time-varying effects are all lost except its average effect. Put in the language of measurement, even though we cannot see the time-variations themselves in the measured oscillator power spectrum, the measured phase noise does reflect the time-varying effects in an averaged sense, and thus, the time-varying effects cannot be ignored in the calculation of phase noise. One example of modifying the averaged diffusion speed via the shape of $\Gamma_{eff}(t)$ is to align ISF with NMF differently, as fully discussed in [12].

The foregoing argument only dealt with a single white noise source. In the presence of multiple uncorrelated white noise sources, it can be easily shown that the overall diffusion constant, D, is sum of all the diffusion constants due to the multiple noise sources. If D_k represents the diffusion constant due to the k-th white noise current, $i_{n,k}$, in Fig. 1 and if there are total M uncorrelated noise sources, the overall diffusion constant, D, is given by

$$\begin{aligned} D &= \sum_{k=1}^{M} D_k \\ &= \sum_{k=1}^{M} \frac{1}{4q_{max}^2} \cdot \frac{\overline{i_{n,k}^2}}{\Delta f} \cdot \Gamma_{eff,k,rms}^2 \end{aligned} \tag{17}$$

where $\Gamma_{eff,k}$ is the effective ISF associated with the k-th white noise current. Combining (17) and (5), we see that the phase noise model this work predicts is commensurate with the phase noise model in [12] [34]. The emphasis in this section was on illuminating the time-varying effects in the context of phase diffusion.

The virtual damping rate, D, in (17) looks rather complicated and hence its physical interpretation is still needed to understand the phase noise phenomenon better. The following section is devoted to this physical interpretation.

V. Physics of Phase Noise

The key to a meaningful interpretation of the virtual damping rate, or the phase diffusion constant, D, is to note that the rate of any diffusion process is determined by two essential elements affecting the process: the *sensitivity* of the physical quantity undergoing the diffusion and the *friction* (energy loss) of the environment in which the diffusion process occurs. This important notion is perfectly captured in the Einstein relation, which he derived to explain Brownian motion [36] [37]. We will begin with a brief introduction to the Einstein relation in the context of Brownian motion. This mechanical example facilitates intuitive understanding, appealing to our everyday experience (*e.g.*, an ink droplet in water).

A. Einstein Relation in Brownian Motion

A Brownian particle of mass, m, immersed in a liquid at temperature, T, with frictional coefficient of γ shown in Fig. 12 undergoes a diffusion process. This is because the Brownian particle walks randomly, incessantly bombarded by thermally agitated liquid molecules. When the random
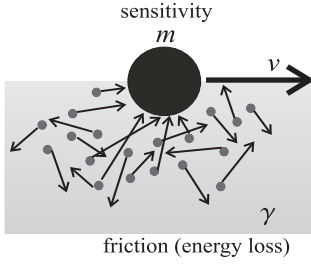
Fig. 12. Brownian motion.

force exerted by the liquid molecules has a white spectrum, the variance of the displacement, x, of the Brownian particle increases proportionally with time, *i.e.*, $\langle x^2 \rangle = 2Dt$, where D is the diffusion constant [18] [19] [37]. This is a key signature of any diffusion process subject to white noise, and is analogous to (2) for the phase diffusion case.

The diffusion constant, D, of the Brownian particle is given by the Einstein relation[8] [18] [19] [37] :

$$D = \underbrace{\frac{k_B T}{m}}_{\text{sensitivity}} \cdot \underbrace{\frac{1}{\gamma}}_{\text{loss}} \qquad (18)$$

where k_B is the Boltzmann constant. The $k_B T/m$ factor represents the *sensitivity* of the Brownian particle to perturbations and becomes smaller for a heavier particle, agreeing with our intuition. Fundamentally, this sensitivity factor derives from the equipartition theorem stating that each independent degree of freedom of a system in equilibrium at temperature T has a mean energy of $k_B T/2$ [19], that is, $\langle mv^2/2 \rangle = k_B T/2$, or $\langle v^2 \rangle = k_B T/m$ where v is the velocity of the Brownian particle.

On the other hand, if two identical Brownian particles with the same mass are immersed in liquids with different frictions, the Brownian particle in a medium with higher friction will exhibit a slower diffusion as we can guess intuitively, and hence the second factor, $1/\gamma$, in (18), originating from the *friction* (*energy loss*) of the environment. Summarizing, the diffusion constant can be determined only when both sensitivity and friction (energy loss) elements are known.

B. Einstein Relation in Phase Noise

The phase diffusion in the oscillator is analogous to the diffusion of the Brownian particle and hence the phase diffusion constant can be also explained using the Einstein relation. To this end, we recast the expression for the phase diffusion constant in (17) into a different form by expressing the noise intensity of the k-th noise current as

$$\frac{\overline{i_{n,k}^2}}{\Delta f} = \frac{4 k_B T}{R_k} \qquad (19)$$

where R_k is the *effective equivalent resistance* associated with the k-th noise current. If the noise is of thermal origin,

[8]In semiconductor physics, the Einstein relation is usually expressed as $D/\mu = k_B T/e$ where μ is mobility [38]. It can be easily shown that this expression is equivalent to (18) [19].

R_k represents the loss associated with the thermal noise according to the fluctuation-dissipation theorem [19], which states the deep-seated link between thermal noise and loss. For instance, in the case of an ohmic resistor, R, such as the tank loss in Fig. 1, R_k simply becomes R and (19) is no more than the Johnson-Nyquist formula for thermal noise. For another example, for the MOS transistor whose channel thermal noise intensity is given by $4 k_B T \gamma g_{d0}$ where γ is the MOS thermal noise factor and g_{d0} is the channel transconductance at $V_{ds} = 0$ [39], R_k is equal to $1/(\gamma g_{d0})$. On the other hand, if the noise is of non-thermal origin (*e.g.*, shot noise), R_k does not necessarily represent the loss since the fluctuation-dissipation relation only holds true for the thermal noise sources. In this case, R_k can be simply thought of as an alternative measure of the noise intensity in the form of resistance.

By plugging (19) into (17) and ignoring the time-varying effects for simplicity, we obtain

$$D = \frac{1}{V_0^2} \cdot \frac{k_B T}{C} \cdot \sum_{k=1}^{M} \frac{1}{R_k C} \qquad (20)$$

where we have also used $q_{max} = CV_0$ of (11). Now we will demonstrate this phase diffusion constant as the Einstein relation.

First, let us consider the diffusion constant only due to the thermal noise of the tank loss, R, in Fig. 1. From now on, we will always reserve the index, $k = 1$, for the tank loss, that is, $R_1 = R$. Then the diffusion constant due to the tank loss is given by

$$D_1 = \frac{1}{V_0^2} \cdot \underbrace{\frac{k_B T}{C}}_{\text{sensitivity}} \cdot \underbrace{\frac{\omega_0}{Q}}_{\text{loss}} \qquad (21)$$

where Q is the *unloaded tank quality factor* defined in (8).

In (21), the $k_B T/C$ factor represents the sensitivity of the tank, analogous to the $k_B T/m$ sensitivity factor of the Brownian particle in (18). This sensitivity factor can be obtained resorting to the equipartition theorem [19] again, that is, $\langle CV^2/2 \rangle = k_B T/2$ or, $\langle V^2 \rangle = k_B T/C$. At the same time, the ω_0/Q factor in (21) is analogous to the $1/\gamma$ factor in (18) for the Brownian motion and is associated with energy loss as the quality factor obviously indicates. These sensitivity and energy loss elements in the phase diffusion constant prove the direct correspondence between the Einstein relation and the phase diffusion constant. The additional factor, $1/V_0^2$, in (21) is simply to convert the diffusion on the limit cycle to the diffusion in the phase angle (*e.g.* Fig. 11).

Now, let us consider the overall phase diffusion constant, D, in Fig. 1. We first define the *loaded resistance*, R_{loaded}, as

$$R_{loaded} \equiv R_1 || R_2 || \cdots || R_M \qquad (22)$$

where R_1 is the tank loss, R, as mentioned shortly before. Then, we can rewrite the phase diffusion constant in (20) as

$$D = \frac{1}{V_0^2} \cdot \frac{k_B T}{C} \cdot \frac{\omega_0}{R_{loaded} C \omega_0} \qquad (23)$$

Comparing this overall diffusion constant to the diffusion constant only due to the tank loss in (21), one can see that the loading effect of the active devices is reflected via the change from R to R_{loaded}. Accordingly, we define the loaded tank quality factor, Q_{loaded}, as

$$Q_{loaded} \equiv R_{loaded} C \omega_0 \qquad (24)$$

simplifying (23) to

$$D = \frac{1}{V_0^2} \cdot \underbrace{\frac{k_B T}{C}}_{\text{sensitivity}} \cdot \underbrace{\frac{\omega_0}{Q_{loaded}}}_{\text{loss/noise}} \qquad (25)$$

Note that Q_{loaded} defined above in the oscillator context is different from the conventional definition of Q_{loaded} in the context of linear time-invariant (LTI) circuits such as tuned-tank amplifiers. Conventionally, the loaded quality factor refers to the overall quality factor taking into account all the relevant circuit parasitics.

As can be seen from (19), (22) and (24), Q_{loaded} defined here is a direct measure of the amount of noise in the oscillator. If all the noise sources are of thermal origin in Fig. 1, Q_{loaded} is a measure of energy loss in the circuit due to the connection between thermal noise and loss (the fluctuation-dissipation theorem). At any rate, ω_0/Q_{loaded} in (25) consists of noise and/or loss elements while $k_B T/C$ in the equation is the sensitivity factor, hence demonstrating the direct correspondence between the Einstein relation and the overall phase diffusion constant.

In this subsection, we identified the two key components determining the oscillator phase noise using a simple physical argument; apart from the $1/V_0^2$ factor, the phase noise is determined by the sensitivity of the resonator and the overall circuit noise represented by the ω_0/Q_{loaded} factor, in perfect agreement with our intuition. Although in this paper the Einstein relation was used as a means of interpreting phase noise, the Einstein relation in the phase diffusion is so fundamental that the phase noise formula can be directly obtained through a cogent physical argument utilizing the Einstein relation, without going through the mathematical derivation in Section IV [40].

C. NCR vs. Phase Noise

Using the definition of noise-to-carrier ratio (NCR) in (9), we can rewrite (25) as

$$D = \frac{E_{thermal}}{E_{tank}} \cdot \frac{\omega_0}{Q_{loaded}} = [\text{NCR}] \cdot \frac{\omega_0}{Q_{loaded}} \qquad (26)$$

where the thermal energy and the tank energy of the oscillator are given by $E_{thermal} = k_B T/2$ and $E_{tank} = C V_0^2/2$, respectively, as mentioned earlier. Although there have recently been emphases on the importance of the NCR in design of oscillators [30] [32] [33], the link between the phase noise and the NCR has not been clearly explained. Now, the above equation in association with the Einstein relation elucidates the link, spelling out that the NCR originates from the sensitivity factor, $k_B T/C$, and the $1/V_0^2$ factor

which converts the diffusion on the limit cycle to the diffusion in the phase angle. As shown in (26), phase noise and the NCR are connected through the ω_0/Q_{loaded} factor which represents the overall noise in the oscillator.

Often in the NCR, only the $1/V_0^2$ factor is emphasized while the $k_B T/C$ factor is neglected, leading to the widely-held belief that a larger oscillator amplitude always results in a better phase noise. However, as can be seen in (26), what actually matters to reduce the NCR is not V_0 alone but E_{tank} determined by both C and V_0. If C is already fixed, every effort should be made to maximize V_0 in the design. If both C and V_0 are the design variables, for a given tank energy, increasing C and thus decreasing V_0 does *not* worsen the NCR. Therefore, if increasing C can benefit the extra ω_0/Q_{loaded} factor in (26), C must be increased (and hence V_0 must be decreased) to improve the phase noise [30].

D. Fluctuation-based and Dissipation-based Phase Noise Models

Using the relation in (19), we were able to express the same phase diffusion constant either in the fluctuation-based form (17) or in the dissipation-based form (25). As mentioned earlier, the fluctuation-based form (17) is commensurate with the model of [12]. On the other hand, it can be shown that the dissipation-based form (25) is equivalent to the familiar Leeson model [7]. By using $Q_{loaded} \sim \omega_0 E_{tank}/P_s = \omega_0 C V_0^2/(2P_s)$ in (25) where P_s is the power dissipation in the resistive part of the resonator, we can rewrite (25) as

$$D \sim \frac{k_B T}{P_s} \cdot \frac{\omega_0^2}{Q_{loaded}^2} \qquad (27)$$

which in conjunction with (5) leads to the Leeson model. This consideration hence establishes a clear link between fluctuation-based phase noise models such as [12] and dissipation-based phase noise models such as [7]. While apparently very different, they are indeed not contradictory but complementary expressions both describing the same physical phase diffusion process.

VI. LINEWIDTH COMPRESSION REVISITED

In Section III, we introduced the concept of the linewidth compression. By comparing the damping rate of the resonator to the virtual damping rate of the oscillator as in Fig. 10, we obtained the linewidth compression ratio given by (7). This ratio is a measure of how much linewidth compression is achieved in placing a resonator into a positive feedback loop. By plugging (25) into (7), we can now explicitly write the linewidth compression ratio in terms of circuit parameters:

$$
\begin{aligned}
r &\sim \frac{1}{V_0^2} \cdot \frac{k_B T}{C} \cdot \frac{Q}{Q_{loaded}} \\
&= [\text{NCR}] \cdot \frac{Q}{Q_{loaded}} \qquad (28)
\end{aligned}
$$

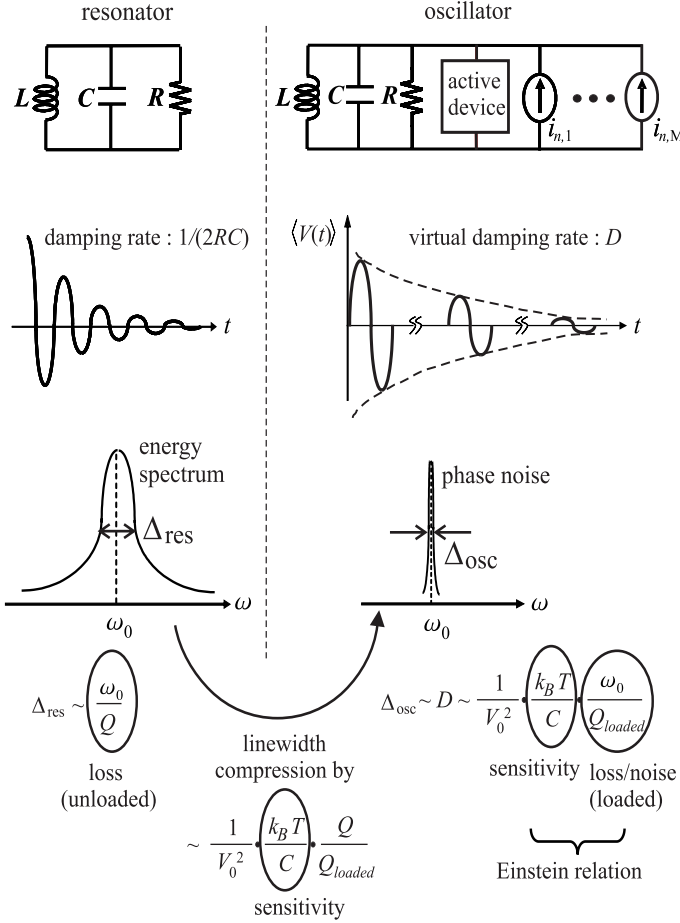where Q is the unloaded tank quality factor defined in (8) and we neglected the numeric proportional constant.

Fig. 13. Anatomy of linewidth compression.

Q_{loaded}, in (24).

VII. Conclusion

This paper presented a new point of view of oscillator phase noise. We introduced the virtual damping concept as a fundamental measure of phase noise along with the experimental verification. The virtual damping concept puts the oscillator phase noise theory and the well-known resonator theory in the same framework, providing a deep and intuitive understanding of linewidth compression. Demonstration of the correspondence between the phase noise and the Einstein relation illuminated the underlying physics of phase noise. These fundamental considerations allowed a meaningful account for the link between the noise-to-carrier ratio (NCR) and the phase noise. Additionally, our fundamental treatment established a link between currently available dissipation-based and fluctuation-based phase noise models.

VIII. Acknowledgment

Appendix

In this appendix, we will demonstrate that the time-varying diffusion equation (13) and the typical diffusion equation (15) lead to the same solution. Plugging the following Gaussian distribution[9]

$$P(\phi, t) = \frac{1}{\sqrt{2\pi\sigma^2(t)}} \exp\left[-\frac{\phi^2}{2\sigma^2(t)}\right] \qquad (29)$$

into the time-varying diffusion equation (13), we obtain

$$
\begin{aligned}
\sigma^2(t) &= \langle \phi^2(t) \rangle \\
&= 2\int_0^t D(t')dt' \\
&= \frac{N}{2C^2V_0^2}(\Gamma_{eff,rms}^2 \cdot t + [\sin/\cos \text{ terms}]) \\
&\approx \frac{N}{2C^2V_0^2}\Gamma_{eff,rms}^2 \cdot t \\
&= 2 \cdot \overline{D(t)} \cdot t \qquad (30)
\end{aligned}
$$

where $\Gamma_{eff,rms}$ signifies the root mean square of the effective ISF. The third line was obtained by decomposing the

Here we will look at the linewidth compression once again, now in connection with the Einstein relation. As already discussed in Section III, the linewidth compression concept shows that the phase noise is determined through a two-step process in the design of the resonator-based oscillator (Fig. 13). In the first step, the resonator's linewidth on the left hand side of Fig. 13 is determined by the unloaded quality factor, Q, of the resonator. This first step is associated with the loss factor in the Einstein relation. In the second step, the resonator's linewidth is compressed by r in (28) when the resonator is placed in the positive feedback loop to make an oscillator, resulting in the final oscillator's linewidth on the right hand side of Fig. 13. As can be seen in (28), this second step is closely related to both the sensitivity factor, k_BT/C, in the Einstein relation, and the voltage swing. Resultantly, the second step of the linewidth compression overall strongly depends on the NCR. This explains the so-far-unclear link between the NCR and the phase noise.

Another factor in the linewidth compression ratio in (28) that deserves discussion is Q/Q_{loaded}. Since the active devices forming the positive feedback loop load the tank, Q in Δ_{res} should be changed to Q_{loaded} in Δ_{osc}, which is taken care of by this Q/Q_{loaded} factor. This justifies the validity of our earlier definition of the loaded tank quality factor,

[9]In this Gaussian distribution, it can be shown that $\langle \phi^2(t) \rangle = \sigma^2(t)$ always holds true. Hence, $\sigma^2(t)$ represents the variance of $\phi(t)$ for a given time t.

time-varying diffusion constant, $D(t)$, into its dc component and non-dc components in the second line. Since in the third line the first term grows unboundedly with time while the sine and cosine terms are bounded, the first term will eventually dominate, leading to the fourth line.

However, the Gaussian distribution in (29) with $\sigma^2(t) = 2 \cdot \overline{D(t)} \cdot t$ in (30) is the solution of the diffusion equation (15) as is well known. Therefore, solving the time-varying diffusion equation (13) and the typical diffusion equation (15) essentially result in the same solution.

References

[1] M. Lax, "Classical noise. V. noise in self-sustained oscillators," *Phys. Rev.,* vol. CAS-160, pp. 290-307, 1967.

[2] R. Kubo, "A stochastic theory of line-shape and relaxation," *Fluctuation, Relaxation and Resonance in Magnetic Systems* (edited by D. Ter Haar), Oliver and Boyd, Edinburgh, 1962.

[3] R. Kubo, "Stochastic Liouville equations," *Journal of Mathematical Physics*, vol. 4, no. 2, pp. 174-183, February 1963.

[4] R. L. Stratonovich, *Topics in the Theory of Random Noise*, vol. II, Gordon and Breach, 1967.

[5] F. K. Kartner, "Analysis of white and $f^{-\alpha}$ noise in oscillators," *Int. J. Circuit Theory Appl.*, vol. 18, pp. 485-519, 1990.

[6] A. Demir, A. Mehrotra, and J. Roychowdhury, "Phase noise in oscillators: a unifying theory and numerical methods for characterization," *IEEE Trans. on Circuits and Systems-I: Fundamental theory and appl.*, vol. 47, no. 5, May 2000.

[7] D. B. Leeson, "A simple model of feedback oscillator noise spectrum," *Proc. IEEE*, vol. 54, pp. 329-330, Feb. 1966.

[8] W. A. Edson, "Noise in oscillators," *Proceedings of IRE*, vol. 48, pp. 1454-1466, August 1960.

[9] B. Razavi, "A study of phase noise in CMOS oscillators," *IEEE Journal of Solid-State Circuits*, vol. 31, no. 3, pp. 331-343, March 1996.

[10] J. J. Rael and A. A. Abidi, "Physical processes of phase noise in differential LC oscillators," *IEEE Custom Integrated Circuits Conference*, Orlando, Florida, May 2000.

[11] K. A. Kouznetsov and R. G. Meyer, "Phase noise in LC oscillators," *IEEE Journal of Solid-State Circuits*, vol. 35, no. 8, August 2000.

[12] A. Hajimiri and T. H. Lee, "A general theory of phase noise in electrical oscillators," *IEEE Solid-State Circuits,* vol. 33, pp. 179-194, February 1998.

[13] E. Hegazi, H. Sjoland, and A. A. Abidi, "A filtering technique to lower LC oscillator phase noise," *IEEE Journal of Solid-State Circuits,* vol. 36, no. 12, December 2001.

[14] M. Straayer, J. Cabanillas, and G. Rebeiz, "A low-noise transformer-based 1.7GHz CMOS VCO," *ISSCC Digest of Technical Papers*, pp. 286 - 287, February 2002.

[15] F. Herzel, "An analytical model for the power spectral density of a voltage-controlled oscillator and its analogy to the laser linewidth theory," *IEEE Transactions on Circuits and Systems-I: Fundamental Theory and Applications,* vol. 45, no. 9, September 1998.

[16] F. Herzel and B. Razavi, "A study of oscillator jitter due to supply and substrate noise," *IEEE Transactions on Circuits and Systems-II: Analog and Digital Signal Processing,* vol. 46, no. 1, January 1999.

[17] A. A. Andronov, A. A. Vitt, and S. E. Khaikin, *Theory of Oscillators*, Oxford, New York, Pergamon Press, 1966.

[18] N. G. Van Kampen, *Stochastic Processes in Physics and Chemistry*, North-Holland Personal Library, 1992.

[19] F. Reif, *Fundamentals of Statistical and Thermal Physics*, McGraw-Hill, 1985.

[20] T. C. Weigandt, B. Kim, and P. R. Gray, "Analysis of timing jitter in CMOS ring oscillators," in *Proc. ISCAS*, May 1994, vol. 4, pp. 27-30.

[21] J. A. McNeill, "Jitter in ring oscillators," *IEEE Journal of Solid-State Circuits*, vol. 32, no. 6, pp. 870-879, June 1997.

[22] A. Hajimiri, S. Limotyrakis, and T. H. Lee, "Jitter and phase noise in ring oscillators," *IEEE Journal of Solid-State Circuits*, vol. 34, no. 6, June 1999.

[23] B. Razavi, *RF Microelectronics*, Prentice-Hall,Inc. 1998

[24] P. Grivet and A. Blaquiere, "Nonlinear effects of noise in electronic clocks," *Proceedings of the IEEE*, pp. 1606-1614, vol. 51, no. 11, November 1963.

[25] B. Razavi, "A 1.8GHz CMOS voltage-controlled oscillator," *ISSCC Digest of Technical Papers*, pp. 388-389, February 1997.

[26] A. Hajimiri and T. H. Lee, "Design issues in CMOS differential LC oscillators," *IEEE Journal of Solid-State Circuits*, vol. 34, no. 5, pp. 717-724, May 1999.

[27] C. Hung and K. O. Kenneth, "A packaged 1.1-GHz CMOS VCO with phase noise of -126dBc/Hz at a 600-kHz offset," *IEEE Journal of Solid-State Circuits*, vol. 35, pp. 100-103, January 2000.

[28] J. Kim and B. Kim, "A low-phase-noise CMOS LC oscillator with a ring structure," *ISSCC Digest of Technical Papers*, pp. 430-431, February 2000.

[29] F. Svelto, S. Deantoni and R. Castello, "A 1.3 GHz low-phase noise fully tunable CMOS LC VCO," *IEEE Journal of Solid-State Circuits*, vol. 35, no. 3, pp. 356-361, March 2000.

[30] D. Ham and A. Hajimiri, "Concepts and methods in optimization of integrated LC VCO," *IEEE Journal of Solid-State Circuits*, vol. 36, no. 6, pp. 896-909, June 2001.

[31] H. Wu and A. Hajimiri, "A 10GHz CMOS distributed voltage controlled oscillator," *IEEE 2000 CICC*, pp. 581-584, May 2000.

[32] Q. Huang, "Phase noise to carrier ratio in LC oscillators," *IEEE Transactions on Circuits and Systems-I: Fundamental Theory and Applications*, vol. 47, no. 7, pp. 965 - 980, July 2000.

[33] T. H. Lee and A. Hajimiri, "Oscillator phase noise: a tutorial," *IEEE Journal of Solid-State Circuits*, vol. 35, no. 3, March 2000.

[34] A. Hajimiri and T. H. Lee, *The Design of Low Noise Oscillators*, Kluwer Academic Publishers, Norwell, Massachusetts. 1999.

[35] D. Ham, *Statistical Electronics: Noise Processes in Integrated Systems*, Ph. D. dissertation, Caltech, 2002.

[36] A. Einstein, *Annalen der Physik* (Leipzig), **17**, 549, 1905.

[37] A. Einstein, *Investigation on the Theory of the Brownian Motion*, Dover Publication, 1956.

[38] S. M. Sze, *Physics of Semiconductor Devices*, 1981, John Wiley & Sons.

[39] A. Van Der Ziel, *Noise in Solid-State Devices and Circuits*, John Wiley & Sons, 1986.

[40] D. Ham and A. Hajimiri, "Virtual damping in oscillators," *IEEE Custom Integrated Circuits Conference*, Orlando, Florida, May 2002.